MOLECULAR AND CELLULAR BIOLOGY, Nov. 2006, p. 8061–8074 Vol. 26, No. 21
0270-7306/06/$08.00+0 doi:10.1128/MCB.01102-06
Copyright © 2006, American Society for Microbiology. All Rights Reserved.

Molecular Architecture of a Eukaryotic DNA Replication Terminus-Terminator Protein Complex▽

Gregor Krings and Deepak Bastia*

Department of Biochemistry and Molecular Biology, Medical University of South Carolina, Charleston, South Carolina 29425

Received 19 June 2006/Returned for modification 17 July 2006/Accepted 21 August 2006

DNA replication forks pause at programmed fork barriers within nontranscribed regions of the ribosomal DNA (rDNA) genes of many eukaryotes to coordinate and regulate replication, transcription, and recombination. The mechanism of eukaryotic fork arrest remains unknown. In *Schizosaccharomyces pombe*, the promiscuous DNA binding protein Sap1 not only causes polar fork arrest at the rDNA fork barrier Ter1 but also regulates *mat1* imprinting at SAS1 without fork pausing. Towards an understanding of eukaryotic fork arrest, we probed the interactions of Sap1 with Ter1 as contrasted with SAS1. The Sap1 dimer bound Ter1 with high affinity at one face of the DNA, contacting successive major grooves. The complex displayed translational symmetry. In contrast, Sap1 subunits approached SAS1 from opposite helical faces, forming a low-affinity complex with mirror image rotational symmetry. The alternate symmetries were reflected in distinct Sap1-induced helical distortions. Importantly, modulating protein-DNA interactions of the fork-proximal Sap1 subunit with the nonnatural binding site DR2 affected blocking efficiency without changes in binding affinity or binding mode but with alterations in Sap1-induced DNA distortion. The results reveal that Sap1-DNA affinity alone is insufficient to account for fork arrest and suggest that Sap1 binding-induced structural changes may result in formation of a competent fork-blocking complex.

DNA replication fork progression is often hampered by strand breaks, damaging DNA lesions, or other types of genotoxic stress. Unless properly protected and/or processed, stalled forks are prone to collapse or regression, thereby potentially leading to genomic instability (reviewed in references 7, 36, and 47). In addition, replication forks also pause at programmed replication fork barriers (RFB, or Ter sites) located in the genomes of many prokaryotes and eukaryotes (reviewed in references 6 and 56). Fork pausing controls diverse biological functions, such as formation of a replication fork trap in the terminus region of circular prokaryotic chromosomes (reviewed in reference 6), regulation of mating-type switching in the fission yeast *Schizosaccharomyces pombe* (15), and proper replication of the tandemly repeated ribosomal DNA (rDNA) genes in yeasts (8, 31, 35, 42, 59, 60, 64). Importantly, programmed fork barriers are recombinogenic and can lead to chromosomal rearrangements (1, 26, 32, 37, 64). In *Saccharomyces cerevisiae*, fork arrest has been implicated in the coordination and regulation of rDNA replication, transcription, and recombination, including the formation of extrachromosomal rDNA circles, which may be implicated in aging (17, 26, 31, 32, 64). Interestingly, fork pausing in the intergenic regions of eukaryotic ribosomal DNA genes has been conserved in yeasts (8, 35, 42, 59, 60), plants (44), *Xenopus laevis* (66), mice (45), and humans (43). Thus, understanding the biochemistry of programmed replication fork arrest within eukaryotic rDNA is likely to be central to understanding rDNA physiology and the maintenance of genome stability within this highly repetitive gene cluster.

Termination of DNA replication has been well studied for prokaryotes (reviewed in references 6, 10, and 53). Thorough analysis of protein-DNA and protein-protein interactions, as well as cocrystal structures of terminator protein-DNA complexes, have generated a wealth of information leading towards an understanding of the mechanism of fork arrest in these systems (11, 27, 38, 51, 52, 58, 62, 67). The site-specific DNA binding terminator proteins Tus and RTP of *Escherichia coli* and *Bacillus subtilis*, respectively, form asymmetric protein-DNA complexes and arrest the oncoming replisome by preventing DNA unwinding by the replicative helicase. Fork arrest is polar or orientation specific, arresting only forks approaching the site from one direction, and this polarity is apparently generated by direct interaction of the functionally asymmetric terminator protein with the replicative helicase (46, 52). Site-specific fork arrest has also been described for various eukaryotic systems (reviewed in references 6 and 56). In *S. cerevisiae*, the protein Fob1 binds to two sites, Ter1 (RFB1) and Ter2, located within the rDNA intergenic spacer to cause polar fork arrest (30, 50). Similarly, the murine RNA polymerase I transcription terminator and the homologous Reb1 of *S. pombe* have been shown to cause fork arrest in the intergenic regions of mouse and fission yeast rDNA, respectively (22, 60). Although several recent studies have addressed the complex regulation of *S. cerevisiae* fork arrest in vivo (12, 20, 49, 65), biochemical analysis of eukaryotic fork-blocking complexes is lacking, and therefore the precise mechanism(s) of replisome blockage remains unknown. In fact, aside from crude DNase I footprinting of Fob1 (30) and Reb1 (68) with their respective binding sites, no studies have yet addressed the topology of eukaryotic terminator protein-Ter complexes.

In *S. pombe*, replication forks pause at four defined fork barriers, Ter1-3 (RFB1-3) and RFP4, within the rDNA intergenic spacer region (35, 60). The RNA polymerase I transcrip-

* Corresponding author. Mailing address: Department of Biochemistry and Molecular Biology, Medical University of South Carolina, 173 Ashley Avenue, Charleston, SC 29425. Phone: (843) 792-0491. Fax: (843) 792-8568. E-mail: bastia@musc.edu.

▽ Published ahead of print on 28 August 2006.

tion terminator Reb1 arrests replication at Ter2 and Ter3 (60), whereas the switch-activating protein Sap1 binds to Ter1 to cause polar fork arrest at this site (34, 48). Sap1 is a multifunctional DNA binding protein, first identified by its binding to a site, SAS1, located centromere proximal to the mating-type switching locus *mat1*, which is required for mating-type switching (4). However, as contrasted with Ter1, Sap1 does not block replication at SAS1 (28, 34). Subsequent studies established that Sap1 is required for viability independently of its function in mating-type switching (2), being required also for maintenance of genome stability. These functions may require, at least in part, Sap1 binding to DNA without sequence specificity (18). In addition, a reiterative screening procedure has identified preferred synthetic Sap1 binding sites, consisting mostly of directly or indirectly repeated core TAA/GCG core motifs (23). Thus, Sap1 appears to be a rather promiscuous DNA binding protein involved in diverse biological functions.

Because analysis of terminator protein-DNA interactions has contributed to understanding fork arrest in prokaryotes, we wished to extend this type of analysis to the study of eukaryotic fork arrest in the rDNA intergenic spacer. We have used a variety of protein-DNA interaction techniques to probe the interaction of Sap1 with Ter1 as contrasted with SAS1. The results yield for the first time significant insight into the architecture of a eukaryotic fork-blocking complex and are compared to the strikingly different architecture of the Sap1-SAS1 imprinting complex. Upon DNA binding, Sap1 causes distinct local helical distortions, which mirror the architecture of the protein-DNA complex. In addition, we demonstrate by mutational analysis of the nonnatural direct repeat-type Sap1 binding site DR2 that modulating the interaction of the fork-proximal subunit of the Sap1 dimer converts this site from an inefficient to an efficient fork barrier in vivo without affecting the affinity of the dimer for the DNA. Local structural changes in the binding site accompany this conversion. The potential biological and mechanistic relevance of the findings is discussed below.

MATERIALS AND METHODS

Protein expression and purification. Wild-type and truncated His_6-Sap1 mutant proteins were expressed in *E. coli* BL21(DE3)(plysS) and purified as previously described (34).

Preparation of substrates for DNA-protein interaction studies. All binding sites were PCR amplified with Vent polymerase (New England Biolabs) from pTer1(IRT2), pDR2(IRT2), pSAS1(IRT2), and the indicated mutant sites (34) to yield fragments of ~160 bp in length. The PCR products were eluted from agarose gels and ~500 ng (~5 pmol) was treated with Optikinase (USB) and [γ-^{32}P]ATP (3,000 Ci/mmol; Perkin-Elmer) according to the manufacturer's instructions. Excess [γ-^{32}P]ATP was removed with Sephadex G-25, and the radiolabeled products were restricted with either AscI or EagI to yield products labeled exclusively on either the top or the bottom strand, respectively. The digested products were desalted using Sephadex G-25. Sequences of all primers and plasmids used are available upon request.

DNase I footprinting. For DNase I footprinting reactions, 30 fmol of wild-type or mutant Ter1- or SAS1-containing fragments (prepared as described above) was incubated with or without His_6-Sap1 for 15 min at room temperature in Sap1 binding buffer (10 mM HEPES, pH 8.0, 100 mM NaCl, 7 mM β-mercaptoethanol, 0.05% Triton X-100, 5% glycerol) containing 2.5 mM $MgCl_2$ and 0.5 mM $CaCl_2$. All reactions were performed in 10-μl volumes and contained 200 ng sheared salmon sperm carrier DNA. DNase I (0.015 U; New England Biolabs) was added for 2 min at room temperature. Reactions were stopped with 100 μl phenol and were immediately vortexed for 10 s and chilled on ice. The aqueous volume was adjusted to 100 μl with 20 mM EDTA and extracted, and the DNA was precipitated with ethanol and glycogen (Sigma), washed with 70% ethanol, and electrophoresed through 8% polyacrylamide-7 M urea sequencing gels containing 30% formamide (to avoid compression artifacts). Gels were dried and exposed to Biomax MS autoradiography film (Kodak).

Missing base contact interference. Missing base contact interference assays (9) were performed using either formic acid (depurination; Sigma) or hydrazine (depyrimidation; Fisher Scientific) as follows. For depurination reactions, 500 fmol (50 ng) of precut Ter1-, DR2-, or SAS1-containing fragments (prepared as described above) was incubated with 1 μl 4% formic acid in the presence of 1 μg sheared salmon sperm carrier DNA in a volume of 10 μl for 30 min at 37°C. The modified DNA was ethanol precipitated, washed with 70% ethanol, and resuspended in 10 μl distilled water. Three reaction mixtures were pooled, and binding reactions were performed using 6 μl modified DNA and 150 to 300 ng His_6-Sap1 in Sap1 binding buffer (10 mM HEPES, pH 8.0, 100 mM NaCl, 7 mM β-mercaptoethanol, 0.05% Triton X-100, 5% glycerol). The amount of protein was sufficient to bind the entire probe in the absence of any modifications. Binding was allowed to proceed for 15 min at room temperature. The reaction mixtures were electrophoresed through 5% native acrylamide gels containing 2.5% glycerol and 0.5× Tris-borate-EDTA (TBE). Bound and unbound bands were excised from the gel and purified using QIAGEN columns according to the manufacturer's instructions. Purified DNA was subsequently cleaved with 1 M piperidine for 30 min at 90°C and precipitated with *n*-butanol. Equal amounts of radioactivity were electrophoresed through 8% polyacrylamide-7 M urea sequencing gels containing 30% formamide. Gels were dried and exposed to Biomax MS autoradiography film (Kodak). Depyrimidation reactions were performed similarly, excepting that the DNA was modified with 30 μl hydrazine for 30 min at room temperature.

DMS protection. For dimethyl sulfate (DMS) protection assays, 30 fmol end-labeled substrates (prepared as described above) was incubated with indicated amounts of His_6-Sap1 for 10 min at room temperature in Sap1 binding buffer (10 mM HEPES, pH 8.0, 100 mM NaCl, 7 mM β-mercaptoethanol, 0.05% Triton X-100, 5% glycerol) containing 400 ng salmon sperm DNA. Binding volumes were 20 μl. Guanines were subsequently methylated by addition of 1 μl of 10% dimethyl sulfate (Sigma) for 2 min, and reactions were stopped by the addition of ammonium acetate to a 2 M final concentration and 2 volumes of ethanol. Modified DNA was precipitated, washed with 70% ethanol, and dried under vacuum. Cleavage at modified bases was performed by the addition of 100 μl 1.5 M piperidine and incubation at 90°C for 30 min, followed by precipitation with *n*-butanol. The dried DNA was resuspended in formamide loading buffer, boiled and chilled, and electrophoresed through 7 M urea-8% acrylamide sequencing gels containing 30% formamide. Gels were dried and exposed to Biomax MS autoradiography film (Kodak).

Hydroxyl radical protection. For hydroxyl radical protection assays, 15 fmol of end-labeled substrates (prepared as described above) was incubated with indicated amounts of His_6-Sap1 for 15 min at room temperature in Sap1 binding buffer lacking glycerol and containing 400 ng salmon sperm DNA. Binding reaction volumes were 20 μl. To the binding reaction mixtures were added 1.5 μl of a 5 mM Fe-10 mM EDTA solution, 1.5 μl of 0.5 mM ascorbate, and 1 μl of 30% H_2O_2 for 4 min at room temperature, and the reactions were stopped with 75 μl of 100 mM thiourea-250 mM EDTA, followed by phenol extraction and ethanol precipitation. Precipitated DNA was washed once with 70% ethanol, dried thoroughly, and electrophoresed through 12% acrylamide-7 M urea sequencing gels containing 20% formamide. Gels were dried and exposed to Biomax MS autoradiography film (Kodak).

Ethylation interference. Ethylation interference assays were performed essentially as described previously (54). Briefly, 4.5 pmol of end-labeled substrates (prepared as described above) was brought to a 100-μl volume in 50 mM sodium cacodylate buffer. An equal volume of saturated ethyl nitrosourea (1 g/5 ml ethanol; Sigma) was added, and the mixture was incubated at room temperature for 30 min, followed by two rounds of ethanol precipitation in the presence of glycogen and subsequent washing with 70% ethanol. The precipitated nucleic acids were dissolved in 10 mM Tris, pH 8.0, and 1 mM EDTA and incubated with the indicated amounts of His_6-Sap1 for 15 min at room temperature in Sap1 binding buffer (10 mM HEPES, pH 8.0, 100 mM NaCl, 7 mM β-mercaptoethanol, 0.05% Triton X-100, 5% glycerol) containing 400 ng salmon sperm DNA. Binding volumes were 20 μl. The reaction mixtures were electrophoresed through 5% native acrylamide gels containing 2.5% glycerol and 0.5× TBE. Bound and unbound fractions were excised, and the DNA was cleaved at ethylated sites by the addition of sodium hydroxide to 150 mM for 30 min at 90°C. Cleavage reaction mixtures were neutralized with acetic acid (to 150 mM), ethanol precipitated, washed with 70% ethanol, and electrophoresed through 12% acrylamide-7 M urea sequencing gels containing 20% formamide. Gels were dried and exposed to Biomax MS autoradiography film (Kodak).

Potassium permanganate probing. Determination of sensitivities of His_6-Sap1-bound binding sites to potassium permanganate ($KMnO_4$) oxidation was performed essentially as described previously (13). Briefly, end-labeled substrates (prepared as described above) were incubated with indicated amounts of His_6-Sap1 for 15 min at room temperature in Sap1 binding buffer lacking reducing agents and containing 400 ng salmon sperm DNA in 20-μl reaction volumes. Subsequently, 2 μl of 50 mM $KMnO_4$ was added for 2 min at room temperature, after which the reaction mixtures were quenched by the addition of 2 μl β-mercaptoethanol. The DNA was ethanol precipitated in the presence of glycogen, washed with 70% ethanol, and cleaved by the addition of 150 μl of 1 M piperidine for 30 min at 90°C. Cleaved DNA was precipitated with *n*-butanol and resolved through 8% acrylamide-7 M urea sequencing gels containing 30% formamide. Gels were dried and exposed to Biomax MS autoradiography film (Kodak).

Comparative gel mobility shift assays. Gel mobility shift assays, used to determine the relative affinities of His_6-Sap1 for its various binding sites, were performed essentially as described previously (34), except for the following minor modifications. DNA probes containing the indicated binding sites were amplified from the respective plasmids, purified, and radiolabeled as described above and subsequently digested with KpnI followed by ethanol precipitation to yield substrates labeled only on the bottom strand. His_6-Sap1 was diluted into buffer containing 10 mM HEPES, pH 8.0, 60 mM KCl, 1 mM dithiothreitol, 5 mM $MgCl_2$, 100 μg/ml bovine serum albumin, and 50% glycerol. Binding reactions were performed in 20-μl reaction volumes containing 12 mM HEPES, pH 8.0, 100 mM NaCl, 50 μg/ml bovine serum albumin, and 7 mM β-mercaptoethanol for 15 min at room temperature, followed by electrophoresis through 7.5% native acrylamide gels containing 2.5% glycerol and 0.5× TBE. Gels were directly exposed to phosphorimager screens at room temperature for 3 to 4 h for quantification of bound and unbound fractions.

2D agarose gel electrophoresis. Preparation and separation of replication intermediates by two-dimensional (2D) gel electrophoresis were performed as described previously (25, 35). In all cases, PvuII-digested plasmid intermediates were probed with a 2.2-kb fragment of the LEU2 gene.

RESULTS

Sequence heterogeneity of the Ter1 and SAS1 sites. Various Sap1 binding sites, including the only known in vivo sites, Ter1 and SAS1, share sequence elements but in differing arrangements (Fig. 1A), as previously reported (23, 34, 48). Specifically, SAS1 contains three TAA/GCG core recognition motifs (motifs a to c), the last two (motifs b and c) being arranged in an inverted configuration with respect to motif a (Fig. 1A). The motifs are separated internally by 12 bp. Notably, this arrangement does not correspond to any of the preferred synthetic binding sites previously isolated in a reiterative screening assay, which consist primarily of directly repeated or inverted core motifs (23). In contrast to SAS1, Ter1 contains the highly conserved core motif a (TAACG) as well as a presumed but weakly conserved core motif b (CAAGG) arranged as direct repeats separated by 5 bp. This configuration resembles previously identified high-affinity direct repeat binding sites, such as DR2, isolated in the reiterative screen mentioned above (23). However, in addition, the site contains a putative inverted motif c (TAGCT) (Fig. 1A). All three motifs are required for Sap1 binding and replication fork arrest (34, 48). Thus, Ter1 contains sequence patterns resembling those of both SAS1 and DR2. It was therefore unclear if and how the varied arrangements of these motifs act to recruit Sap1 to its respective binding sites in differing configurations. Therefore, we wished to determine whether biological function, such as fork arrest, is favored by a specific binding mode, as discussed below.

Distinct patterns of DNase I protection within the Sap1-Ter1 and Sap1-SAS1 complexes. In order to begin to address the functional significance of the heterogeneity of Sap1 binding sites, we performed DNase I protection footprinting assays of

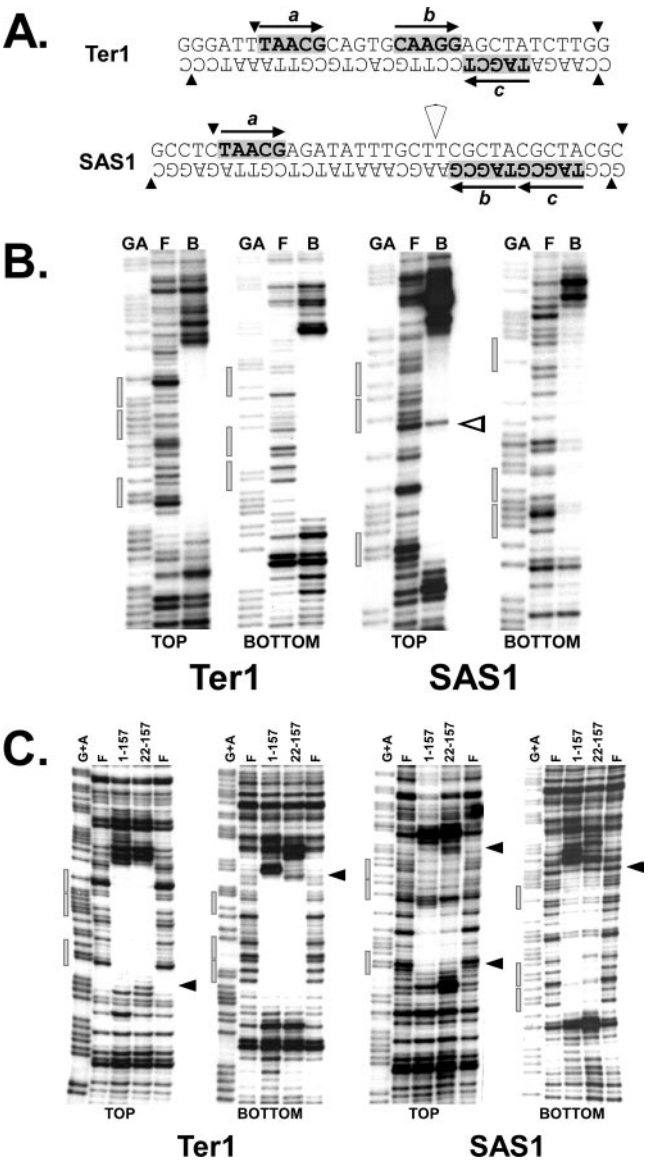

FIG. 1. DNase I footprinting of wild-type and truncated His_6-Sap1 mutants complexed with Ter1 or SAS1. (A) Sequence comparison of Ter1 and SAS1. Sap1 core motifs a, b, and c are highlighted in light gray, and directions of the repeats are depicted by black arrows above and below the sequences. The extent of DNase I protection by wild-type His_6-Sap1 (see below) is denoted by black arrowheads. The white arrowhead above SAS1 between motifs a and b denotes the internal DNase I accessible site. (B) DNase I footprinting of His_6-Sap1 on top and bottom strands of Ter1 and SAS1. The white arrowhead denotes the internal DNase I accessible site in the top strand of complexed SAS1. Locations of the core motifs a to c are denoted by gray boxes. All lanes contain 30 fmol Ter1 or SAS1. Lanes GA, G+A Maxam-Gilbert sequencing ladder; lanes F, uncomplexed (free) DNA probe; lanes B, DNA probe plus 40 ng (Ter1) or 60 ng (SAS1) His_6-Sap1. (C) DNase I footprinting of His_6-Sap1(1–157) and His_6-Sap1(22–157) truncation mutants on the top and bottom strands of Ter1 and SAS1. Each lane contains 30 fmol DNA probe. Black arrowheads denote regions of decreased protection of Ter1 or SAS1 by the Sap1(22–157) mutant compared to the Sap1(1–157) mutant (and wild-type) protein. Lanes 3, DNA probe plus 50 ng (Ter1) or 100 ng (SAS1) His_6-Sap1(1–157); lanes 4, DNA probe plus 50 ng (Ter1) or 100 ng (SAS1) His_6-Sap1(22–157). Other lanes are defined above.

recombinant His_6-Sap1 bound to either Ter1 or SAS1 (Fig. 1B). Sap1 protected ~25 and ~30 bp on the top and bottom strands of Ter1, respectively, from DNase I cleavage under the conditions used. As expected, all three core motifs were protected (Fig. 1B). In contrast, Sap1 protected ~30 and ~35 bp on the top and bottom strands of SAS1, respectively (Fig. 1B), providing initial clues that the two complexes differ in mode of Sap1 binding. Importantly, we found reactivity internal to SAS1 (Fig. 1A and B), which was absent in Ter1, revealing that DNase I has access to the minor groove in this region. These results suggested that the Sap1 dimer forms a more compact complex on Ter1 than on SAS1.

In order to further examine differences in the two complexes, we expressed and purified two His_6-Sap1 truncations, Sap1(1–157) (with residues 1 to 157 deleted) and Sap1(22–157), for use in DNase I protection assays. These truncations were chosen for analysis as they retain the DNA binding domain as well as a region of the coiled C-terminal dimerization domain and have been shown to remain functional for SAS1 dimer binding as demonstrated by gel mobility shift assay (3, 23). The results of the footprinting experiments suggest that the Sap1(1–157) truncation and the wild-type protein protect similar regions of Ter1 and SAS1 from DNase I cleavage (Fig. 1C). In contrast, the Sap1(22–157) truncation, which lacks the ill-defined N-terminal domain presumed to mediate alternative protein dimerization in the absence of the C-terminal domain (23), reveals patterns of protection different from those of the wild-type and Sap1(1–157) proteins on both Ter1 and SAS1. Significantly, the patterns of protection differ also between Ter1 and SAS1 (Fig. 1C). Sap1(22–157) allowed for increased DNase I access to Ter1 in the region of the proximal core motif a on both the top and the bottom strand (Fig. 1C) but not in the distal region adjacent to motif c. In contrast, although both truncations bound SAS1 less tightly than Ter1, it was clear that Sap1(22–157) allowed increased DNase I access from both the proximal and the distal side of SAS1 on both strands (Fig. 1C). In summary, the DNase I footprinting results suggest that the Sap1-Ter1 and Sap1-SAS1 complexes exist as structurally distinct complexes. Experiments with the truncation mutants suggest that the N-terminal domain of at least one Sap1 subunit may reside in the vicinity of the proximal core motif a of Ter1. In contrast, the N-terminal domains appear to reside near both the proximal a and the distal c core motif of SAS1. The architectural models built by additional experiments in this paper further support this conclusion (see below).

Contrasting modes of sequence recognition at Ter1 versus SAS1. Identification of terminator protein-base pair contacts has resulted in significant insight into the mechanism(s) of fork arrest in prokaryotes (14, 38, 51, 58, 62). We wished to extend this analysis to the study of eukaryotic fork arrest at Ter1. Additionally, we reasoned that determination of base-specific contacts at Ter1 versus SAS1 should shed further light on the differences between the Sap1 fork-blocking and imprinting complexes, which may result in different biological functions of the complexes. Towards these goals, we performed missing base contact interference as well as DMS protection assays of Sap1 bound to either Ter1 (Fig. 2) or SAS1 (Fig. 3). Missing base contact interference involves the chemical removal of bases in order to determine which bases are required for stable protein binding (9). DMS methylates N^7 of guanine residues and N^3 of adenine residues within the major and minor grooves of the double helix, respectively, and complexes are subsequently assayed for residues that are protected from methylation by the bound protein. Thus, the techniques are complementary for determining base-specific contacts within protein-DNA complexes.

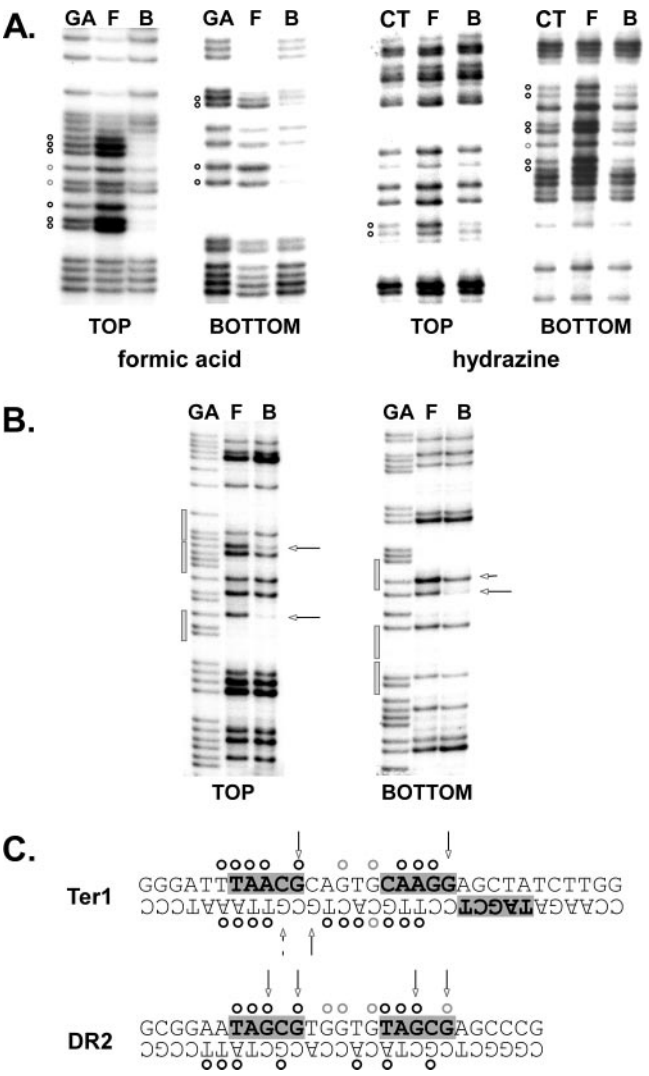

FIG. 2. Base-specific contacts of His_6-Sap1 on Ter1. (A) Representative missing base contact interference gels of top and bottom depurinated (left two panels) and depyrimidated (right two panels) Ter1 sites. Black circles denote bases revealing strong interference when missing, whereas gray circles represent relatively weaker interference. (B) Representative DMS methylation protection gels of top and bottom strands of Ter1. The long white arrows denote regions of strong protection, whereas the short arrow denotes a region of relatively weaker protection. Lanes GA, CT, F, and B denote G+A Maxam-Gilbert sequencing ladders, C+T Maxam-Gilbert sequencing ladders, uncomplexed (free) DNA probe, and complexed (bound) DNA probe, respectively. (C) Summary diagram of His_6-Sap1 base-specific contacts on Ter1 compared to the nonnatural direct-repeat binding site DR2. Core motifs a, b, and c are highlighted in light gray. Symbols are described above.

The results of missing base contact interference analysis and DMS protection of His_6-Sap1 bound to Ter1 are shown in Fig.

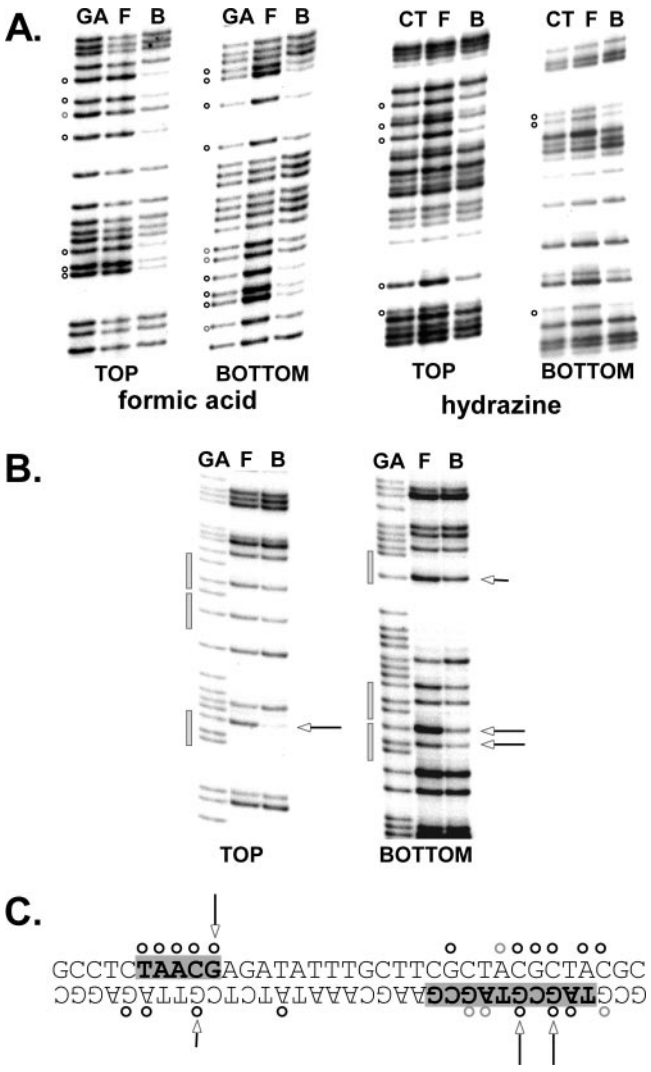

FIG. 3. Base-specific contacts of His_6-Sap1 on SAS1. (A) Representative missing base contact interference gels of top and bottom depurinated (left two panels) and depyrimidated (right two panels) SAS1 sites. (B) Representative DMS methylation protection gels of top and bottom strands of SAS1. (C) Summary diagram of His_6-Sap1 base-specific contacts on SAS1. Symbols and lane designations are described in the legend for Fig. 2.

2A and B, respectively, and are summarized in Fig. 2C. Missing base interference revealed that Sap1 makes specific contacts with both directly repeated core motifs a and b on both strands, resembling contacts made on the direct repeat nonnatural binding site DR2, previously identified through reiterative screening of high-affinity binding sites (23) (Fig. 2C). Similarly, Sap1 protected the terminal guanines of motifs a and b on the top strand, as well as two guanines in the vicinity of motif a on the bottom strand, from DMS methylation (Fig. 2B and C). Because no adenines were protected, we conclude that Sap1 binds Ter1 in successive major grooves and recognizes Ter1 as a direct repeat. Guanines located between motifs a and b in Ter1 (and DR2) were identified by missing base interference to be required for protein binding (Fig. 2A and C) and yet were not protected from methylation (Fig. 2B and C), suggesting that this region probably does not make direct contact with Sap1 but may instead contribute to binding by affecting the architecture of the sugar-phosphate backbone in this region (54). Interestingly, no contacts were detectable at the inverted motif c, although this region is essential for Sap1 binding and fork arrest (48). These results could be reconciled with the fact that the missing base contact interference assay does not necessarily detect cooperative contacts between multiple bases if more than one base is required for binding. Alternatively, this region may contribute to Sap1 binding via an indirect readout mechanism. Regardless, it is clear that the mechanism of site recognition and therefore dimer assembly resembles that of the direct repeat DR2. Notably, no binding asymmetry was detected between the top and bottom strands.

The base-specific contacts of the Sap1-SAS1 complex differed markedly from those at Ter1 (Fig. 3A to C). As is the case for Ter1, Sap1 makes extensive contacts with motif a, as revealed by both missing base interference and DMS protection. However, few missing bases in the inverted motif b affected binding, and no significant methylation protection was observed in this region, suggesting that Sap1 makes few if any base contacts in this region. Instead, removal of bases from inverted motif c affected binding, and methylation protection confirmed that the protein made contact in this region (Fig. 3A to C). As was the case for Ter1, Sap1 appears to make only major-groove contacts with SAS1. Notably, as contrasted with the Sap1-Ter1 complex, we found that only a single base (an adenine on the bottom strand) (Fig. 3A and C) located between the core motifs affected Sap1 binding, perhaps suggesting that this region tolerated alterations in the backbone better than Ter1. This interpretation would be consistent with our DNase I footprinting and DNA bending results (34) suggesting that Sap1 is subject to considerably less space restraint when bound to SAS1 than when bound to Ter1.

In summary, base contacts of Sap1 with Ter1 and SAS1 reveal that the protein makes similar contacts with motif a of both sites. In contrast, directly repeated motif b contributes important base contacts to the Sap1-Ter1 complex, whereas Sap1 contacts primarily the inverted motif c in SAS1. Taken together with our results verifying that a single subunit of the dimer binds motif a of Ter1 (see below), the results suggest that the two complexes differ in sequence recognition and therefore binding configuration of the second but not the first subunit of the dimer and that the arrangement of motifs b and c may direct the mode of binding.

A single Sap1 subunit recognizes motif a of Ter1, and the Sap1 dimer subsequently nucleates at this site. Both the monomeric Tus and dimeric RTP replication terminator proteins of *E. coli* and *B. subtilis*, respectively, have been shown to expose asymmetric faces of the complex to the oncoming replication fork (46, 52). Because Sap1 is a dimer in solution and when bound to DNA (5, 23), we wished to further define the manner by which individual Sap1 subunits recognize and bind Ter1, as asymmetric assembly of the dimer could, in principle, contribute to polar fork arrest. Such asymmetry has been well documented for the cooperative assembly of RTP dimers (38, 41), although other mechanisms must also contribute to polarity generation in this system (19, 46). Towards this goal, we utilized a truncated Sap1 protein, Sap1(1–136), which retains the DNA binding domain but lacks the entire C-terminal

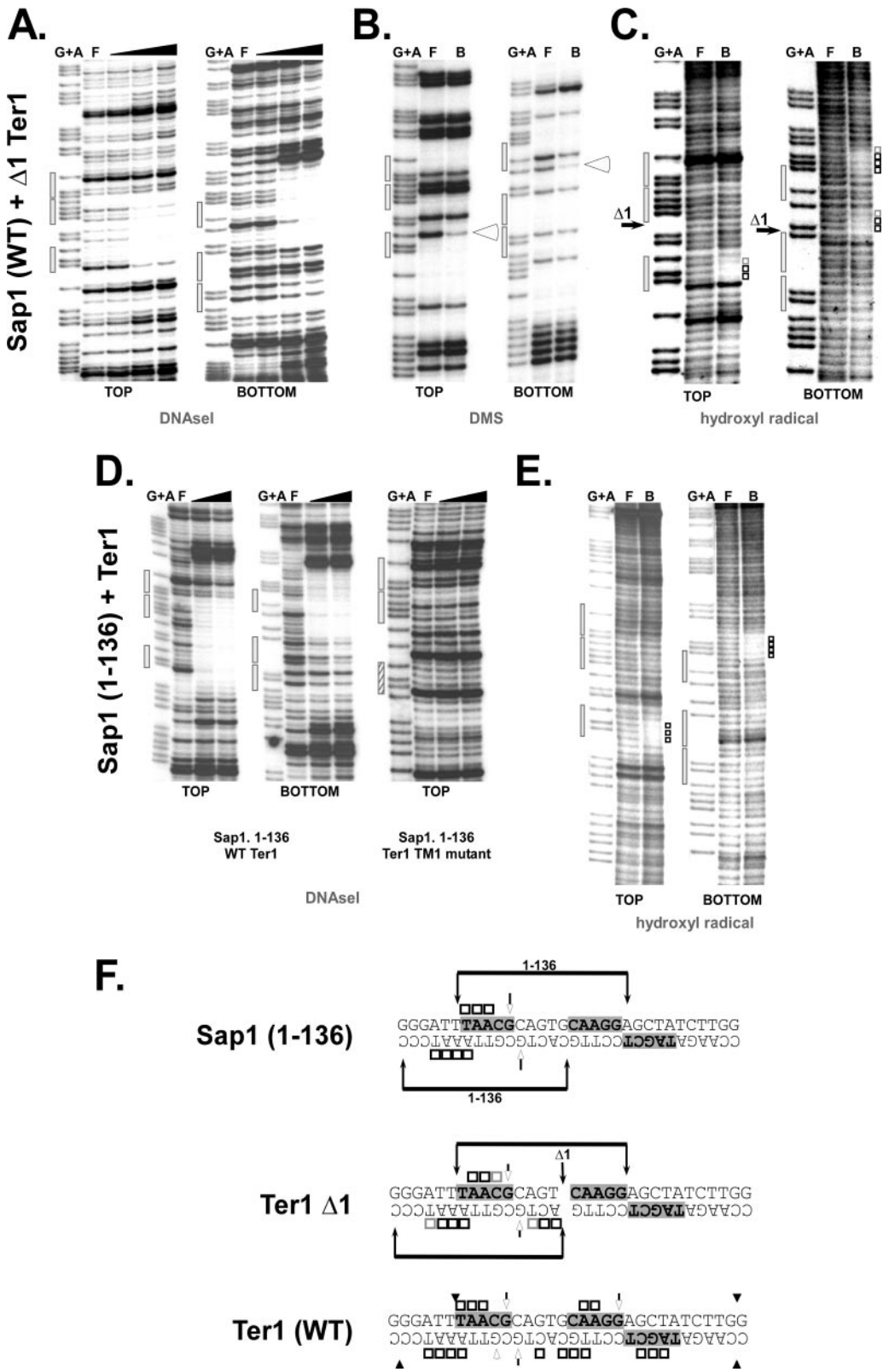

FIG. 4. Motif a of Ter1 acts as a nucleation center for assembly of the Sap1 dimer. (A) DNase I footprints of His_6-Sap1 complexed with the top and bottom strands of the Ter1 Δ1 mutant. All lanes contain 30 fmol Ter1 or Ter mutant DNA. Lanes G+A, Maxam-Gilbert G+A sequencing ladder; lanes F, DNase I-treated uncomplexed (free) Ter1 Δ1 mutant; lanes 3 to 5, DNase I-treated Ter1 Δ1 mutant bound with 10, 50, and 100 ng of His_6-Sap1, respectively. (B) DMS methylation protection of top and bottom strands of the Ter1 Δ1 mutant. All lanes contain 30 fmol Ter1 Δ1 mutant DNA. Lanes F, uncomplexed (free) Ter1 Δ1 mutant; lanes B, Ter1 Δ1 mutant plus 300 ng of His_6-Sap1. White arrowheads denote protected guanines. (C) Hydroxyl radical protection footprints of top and bottom strands of the Ter1 Δ1 mutant in the presence and absence of

dimerization domain and is therefore unable to dimerize properly to form a stable complex on either SAS1 or direct repeat-type binding sites, as determined by gel mobility shift analysis (3, 23). As expected, the mutant is also unable to shift Ter1 in a gel mobility shift assay (data not shown). However, Sap1(1–136) was able to recognize and bind to Ter1, although with reduced affinity, as determined by DNase I footprinting analysis. Significantly, only the proximal one-half of the binding site was occupied by the mutant, even at high protein concentrations (Fig. 4D and F). Using a previously characterized triple mutant of motif a (the TM1 mutant) (34), we detected absolutely no DNase I protection, even at very high protein concentrations (Fig. 4D, right panel). Because the Sap1(1–136) mutant retains the entire DNA binding domain and Sap1 is known to bind Ter1 as a dimer (34), we postulated that the Sap1(1–136) footprint represented the binding of a single Sap1 subunit to Ter1. To gain further support for this notion, we utilized a Ter1 Δ1 mutant, previously shown to be completely defective in stable Sap1 binding as determined by gel mobility shift assay (34). This mutant contains a G deletion immediately preceding motif b (34) (Fig. 4F). DNase I footprinting analysis of wild-type Sap1 on the Ter1 Δ1 mutant resulted in a footprint identical to that of Sap1(1–136) on wild-type Ter1 (compare Fig. 4A and D), suggesting that the dimer can fill only the proximal one-half of Ter1 in the presence of the Δ1 mutation, which presumably prevents recognition of motif b. DMS protection experiments support these results, as guanine residues within only motif a and not motif b are protected by binding of Sap1 to the Δ1 mutant site (Fig. 4B).

Confirming the DNase I and DMS protection results, hydroxyl radical protection assays of wild-type Sap1 on the Ter1 Δ1 mutant and of Sap1(1–136) on wild-type Ter1 reveal that the respective proteins make backbone contacts with sugar-phosphates only in the proximal half of Ter1 (Fig. 4C, E, and F), as contrasted with contacts made by full-length Sap1 on the wild-type Ter1 (Fig. 5A). Minor differences in protection from hydroxyl radical cleavage were noted for the bottom strand. Specifically, additional sugar-phosphates were protected in the Ter1 Δ1 mutant-bound Sap1 complex compared to the wild-type-Ter1-bound Sap1(1–136) complex (Fig. 4C, E, and F). In light of the data as a whole, we interpret these minor differences to perhaps represent conformational differences between the full-length Sap1 dimer and the Sap1(1–136) truncation when bound to motif a, rather than differences in site recognition per se.

The results of these experiments are expected if a single Sap1 subunit contacts Ter1 at motif a, with the second subunit of the dimer subsequently recognizing motif b and binding to motifs b and c. Because binding to motifs b and c requires prior recognition and binding to motif a, we conclude that motif a acts as a nucleation center for dimer binding. Notably, no binding of SAS1 by the Sap1(1–136) mutant was visible by DNase I protection footprinting (data not shown), suggesting that the mechanisms of dimer assembly may differ between the Sap1-Ter1 and Sap1-SAS1 complexes.

Sap1-induced helical distortion. We have demonstrated previously that Sap1 bends both Ter1 and SAS1 upon binding, although bending of Ter1 was reproducibly greater than that of SAS1 (34). These results suggested that the helices were distorted to different extents within the two complexes. As DNA bending and helical distortion are common among bacterial terminators (27, 33) and may contribute to the mechanism of fork arrest in these systems, we were interested to investigate further the Sap1-mediated structural changes at Ter1 and to compare these with the Sap1-SAS1 complex. $KMnO_4$ efficiently oxidizes thymine (and, to a lesser extent, cytosine) bases only when the DNA helix is locally unwound or distorted, and the modified bases subsequently may be detected by piperidine cleavage (61). We therefore probed His_6-Sap1-bound and unbound Ter1 and SAS1 with $KMnO_4$ in order to detect protein-mediated helical distortions at these sites.

Sap1 binding resulted in strand-specific exposure of $KMnO_4$-sensitive bases at Ter1, as only the bottom strand showed hypersensitivity to $KMnO_4$ (Fig. 6A, left two panels). Specifically, the second-position bottom-strand thymine of motif a became reactive after Sap1 binding. In addition, the first-position thymine of the inverted motif c was reactive, although to a greatly reduced extent (Fig. 6A). In addition, a bottom-strand cytosine immediately preceding motif b was reactive (Fig. 6A). Reactivity at this site was severely reduced compared to that of the thymines, but this may be because $KMnO_4$ oxidizes cytosines inefficiently compared to thymines (57). For comparison, we performed similar experiments with the His_6-Sap1-SAS1 complex. As expected, the pattern of Sap1 binding-induced $KMnO_4$ reactivity was strikingly different at this site compared to that at Ter1. Notably, both strands of SAS1 became hypersensitive to $KMnO_4$ upon Sap1 binding (Fig. 6A, right two panels). Although reactivity of the second-position thymine of motif a was analogous to that at Ter1, the reactivities at motifs b and c differed. As with the a motifs of both Ter1 and SAS1, second-position thymines of SAS1 motifs b and c were modified. It should be noted that in each case (motif a of Ter1 and motif a of SAS1, as well as motifs b and c of SAS1), the Sap1-exposed thymines were on the strand opposite the defined TAA/GCG core sequences. This likely reflects the orientation of subunit binding to these motifs, as summarized below. It is interesting to note also that the helical distortion at these bases is exquisitely local, as demonstrated by the

His_6-Sap1. All lanes contain 15 fmol Ter1 Δ1 mutant DNA. Lanes F, uncomplexed (free) Ter1 Δ1 mutant; lanes B, Ter1 Δ1 mutant plus 100 ng of His_6-Sap1. The location of the Δ1 deletion is noted. (D) DNase I footprints of the His_6-Sap1(1–136) truncation mutant complexed with the top and bottom strands of wild-type Ter1 and with the top strand of the Ter1 TM1 triple mutant. All lanes contain 30 fmol DNA. Lanes F, uncomplexed (free) Ter1 (or TM1 mutant); lanes 3 and 4, Ter1 (or TM1 mutant) bound with 200 and 400 ng of His_6-Sap1, respectively (or with 400 and 600 ng of His_6-Sap1 for the TM1 mutant). (E) Hydroxyl radical protection footprints of top and bottom strands of wild-type Ter1 in the presence and absence of His_6-Sap1(1–136). All lanes contain 15 fmol Ter1. Lanes F, uncomplexed (free) Ter1; lanes B, Ter1 bound with 100 ng of the His_6-Sap1(1–136) mutant. (F) Summary diagram of contact data presented in panels A to E. Regions of DNase I protection are indicated with brackets. Small black boxes represent strong protection from hydroxyl radical cleavage, and small gray boxes represent relatively weaker protection. Locations of the core motifs a to c are denoted by long gray boxes. WT, wild type.

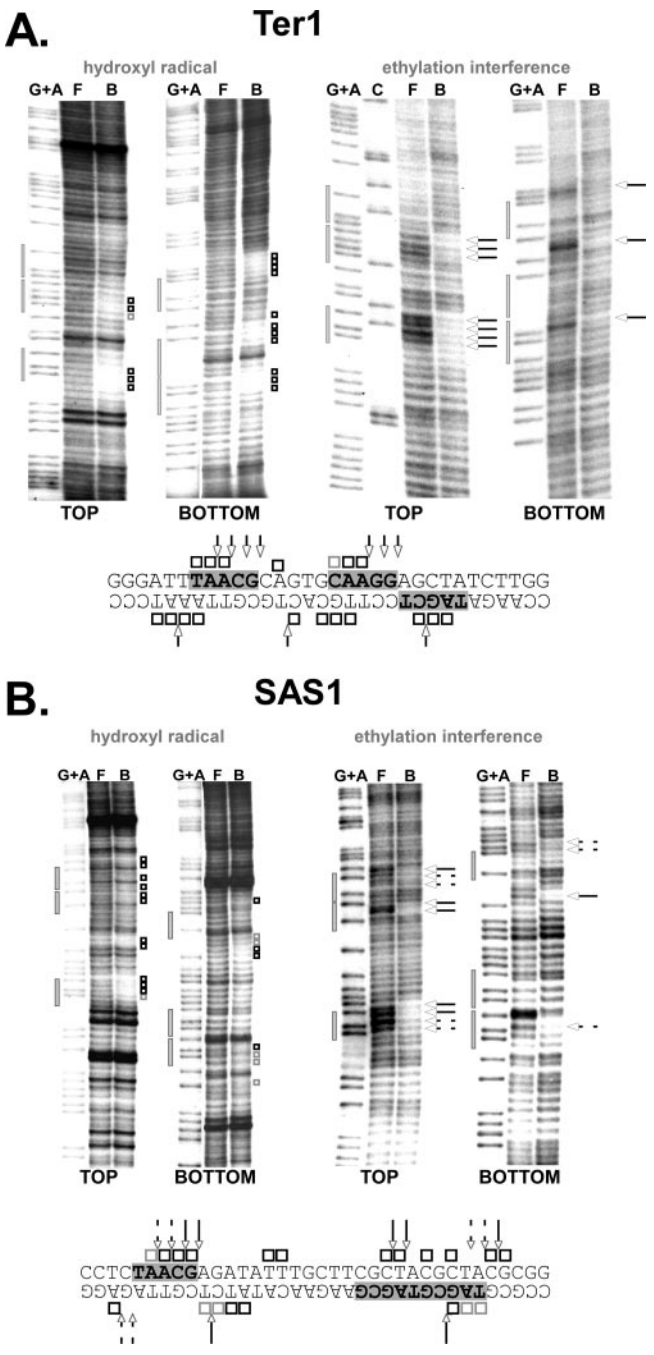

FIG. 5. Sap1 sugar-phosphate backbone contacts at Ter1 and SAS1. (A) (Left two panels) Hydroxyl radical protection footprinting of His_6-Sap1 on the top and bottom strands of Ter1. All lanes contain 15 fmol Ter1. Lanes G+A, G+A Maxam-Gilbert Ter1 sequencing ladder; lanes F, uncomplexed (free) Ter1; lanes B, Ter1 plus 50 ng His_6-Sap1. (Right two panels) Ethylation interference footprinting of His_6-Sap1 on the top and bottom strands of Ter1. Lane C, C Maxam-Gilbert Ter1 sequencing ladder; lanes B, Ter1 plus His_6-Sap1. A diagrammatic representation of Sap1-Ter1 backbone contacts is shown below the panels. (B) (Left two panels) Hydroxyl radical protection footprinting of His_6-Sap1 on the top and bottom strands of SAS1. All lanes contain 15 fmol SAS1. Lanes G+A, G+A Maxam-Gilbert SAS1 sequencing ladder; lanes F, uncomplexed (free) SAS1; lanes B, SAS1 plus 100 ng His_6-Sap1. (Right two panels) Ethylation interference footprinting of His6-Sap1 on the top and bottom strands of SAS1. Lanes B, SAS1 plus His_6-Sap1. A diagrammatic representation of Sap1-SAS1 backbone contacts is shown below the panels. Locations of ethylated phosphate groups that strongly or partially interfere with Sap1 binding are denoted by white solid and hatched arrows, respectively. Locations of the core motifs a to c are denoted by long gray boxes. Locations of strongly and partially protected sugars are denoted by small black and gray boxes, respectively.

$KMnO_4$-insensitive neighboring thymines in the third position of motif a (Fig. 6A and C). In addition to exposure of these motif-embedded thymines, a single top-strand thymine located between motifs b and c of SAS1 became $KMnO_4$ sensitive upon Sap1 binding (Fig. 6A and C).

As summarized in Fig. 6C, the majority of Sap1 binding-induced $KMnO_4$-detectable helical distortions in both SAS1 and Ter1 were located within the core recognition motifs at bases which apparently make direct contact with Sap1. These results were surprising, as we expected dimer-induced bending to result in more-severe distortion of the DNA located between subunit binding regions rather than within them. Indeed, Sap1 dimerization is required for all $KMnO_4$-detectable helical distortion, as binding of the His_6-Sap1(1–136) mutant lacking the well-characterized C-terminal dimerization domain does not result in $KMnO_4$ reactivity at Ter1, whereas binding of both the Sap1(1–157) and the Sap1(22–157) truncated protein does (Fig. 6B). We conclude that Sap1 dimer binding causes radical though different local rearrangements of both Ter1 and SAS1. The potential implications of this site rearrangement for Sap1-mediated fork arrest at Ter1 are discussed below.

Alternate symmetries of the Sap1 terminator and imprinting complexes. We have used a series of footprinting and chemical modification, protection, and interference techniques in order to identify the protein-base pair and protein-backbone contacts of Sap1 at the fork barrier site Ter1 and have contrasted the results with contacts at SAS1. Accordingly, we have been able to describe the molecular architectures of both complexes. The results of these experiments have been synthesized and modeled onto double-helical representations of the respective binding sites, as depicted in Fig. 7. Representation of the data in such a manner allows for visualization of the striking architectural differences between the two functionally distinct complexes.

The Sap1 dimer approaches Ter1 from one face of the DNA helix. A single subunit recognizes motif a and reaches into the major groove here to make base pair contacts while simultaneously making extensive sugar and phosphate contacts with the backbone of this motif (Fig. 2, 4, 5, and 7). It is possible that the terminal two phosphates of motif a identified by ethylation interference footprinting to be required for Sap1 binding are required for binding not because the protein contacts these groups directly but because they are located adjacent to a protected guanine and thus the ethyl group may interfere with Sap1-base pair contacts in this region (Fig. 7). Additional backbone contacts are made by the subunit on the opposite lip of the same major groove (Fig. 4D and 7). After nucleation at motif a (Fig. 4), the second Sap1 subunit makes analogous major-groove base pair and sugar-phosphate contacts with motif b, thus allowing the dimer to bridge the intervening minor groove. Interestingly, we were able to detect only backbone

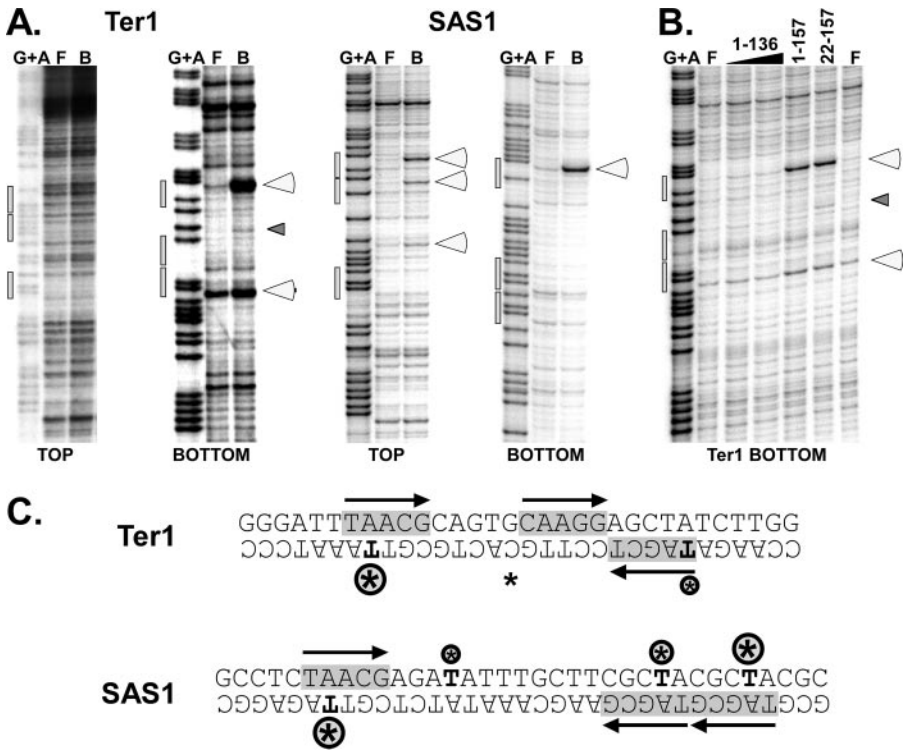

FIG. 6. Sap1 binding causes different patterns of $KMnO_4$-sensitive structural distortions at Ter1 and SAS1. (A) (Left two panels) $KMnO_4$ probing of the top and bottom strands of Ter1 in the presence and absence of His_6-Sap1 binding. All lanes contain 20 fmol Ter1. Lanes G+A, G+A Maxam-Gilbert Ter1 sequencing ladder; lanes F, uncomplexed (free) Ter1; lanes B, Ter1 plus 50 ng His_6-Sap1. (Right two panels) $KMnO_4$ probing of the top and bottom strands of SAS1 in the presence and absence of His_6-Sap1 binding. All lanes contain 20 fmol SAS1. Lanes G+A, G+A Maxam-Gilbert SAS1 sequencing ladder; lanes F, uncomplexed (free) SAS1; lanes B, SAS1 plus 100 ng His_6-Sap1. (B) $KMnO_4$ probing of the bottom strand of Ter1 in the presence or absence of His_6-Sap1 truncation mutants. All lanes contain 20 fmol Ter1. Lane G+A, G+A Maxam-Gilbert Ter1 sequencing ladder; lanes F, uncomplexed (free) Ter1; lanes 3 and 4, Ter1 plus 200 and 400 ng His_6-Sap1(1-136), respectively; lane 5, Ter1 plus 50 ng His_6-Sap1(1–157); lane 6, Ter1 plus 50 ng His_6-Sap1(22–157). Hypersensitive thymines and cytosines are depicted by white and gray arrowheads, respectively. Locations of the core motifs a to c are depicted by gray boxes. (C) Diagrammatic representations of Ter1 and SAS1 pyrimidines that become hypersensitive to $KMnO_4$ oxidation upon His_6-Sap1 binding. Encircled asterisks represent sensitive thymines, and plain asterisks represent sensitive cytosines. The degree of sensitivity is denoted by the size of the respective symbol. Core motifs a, b, and c are highlighted in light gray, and directions of the repeats are depicted by black arrows.

contacts at motif c, which is located on the opposite lip of this major groove and is required for fork-blocking activity (48). In summary, the complex displays obvious translational symmetry, with subunits binding in nearly identical manners to motifs a and b (Fig. 7).

Helical projection of the Sap1-SAS1 complex reveals the stark architectural differences of this complex compared to Sap1-Ter1 (Fig. 7). Base pair and sugar-phosphate contacts at motif a resemble analogous contacts at Ter1, and backbone contacts are also made on the opposite lip of this major groove, suggesting that a single Sap1 subunit binds to this region in a manner similar to that of Ter1. However, motif c appears to contribute most of the remaining base-specific contacts. Furthermore, Sap1 makes extensive sugar-phosphate contacts with motifs b and c from the opposite face of the helix (Fig. 5 and 7). These contacts reveal mirror image symmetry with respect to contacts at motif a, thus providing the complex with rotational symmetry rather than the translational symmetry evident at Ter1 (Fig. 7). Thus, although the C-terminal dimerization domain of Sap1 appears to be required for stable binding of both SAS1 and Ter1 as determined by gel mobility shift assay (23; this study), the second subunit of the dimer appears to be oriented in opposite orientations in the two complexes (Fig. 7 and 8). In addition, the complex accommodates an extra 1.5 helical turns between subunits (Fig. 7). Sap1-induced Ter1 and SAS1 structural distortions mirrored the alternate symmetries of the two complexes (Fig. 6 and 7).

Conversion of the nonnatural Sap1 binding site DR2 into an efficient fork barrier by modulation of the interaction of the fork-proximal Sap1 subunit with Ter1. Having established that Sap1 forms structurally distinct complexes with Ter1 and SAS1 and that Sap1-SAS1 does not arrest replication forks (16, 28, 34), we wished to determine whether the orientation of the dimer on its binding site is sufficient to cause fork pausing. Specifically, does any Sap1 protein-DNA complex with translational symmetry such as Sap1-Ter1 block the fork? Towards this goal, we chose to examine whether the nonnatural direct repeat-type Sap1 binding site DR2 is able to arrest replication in vivo. Replication intermediates of a plasmid containing DR2 cloned in the same orientation as the natural blocking-type Ter1 sequence were isolated and analyzed by 2D agarose electrophoresis. The results show that DR2 was able to act only as a very inefficient fork barrier in vivo (Fig. 8B).

Because the sequences of Ter1 and DR2 (Fig. 8A) as well as

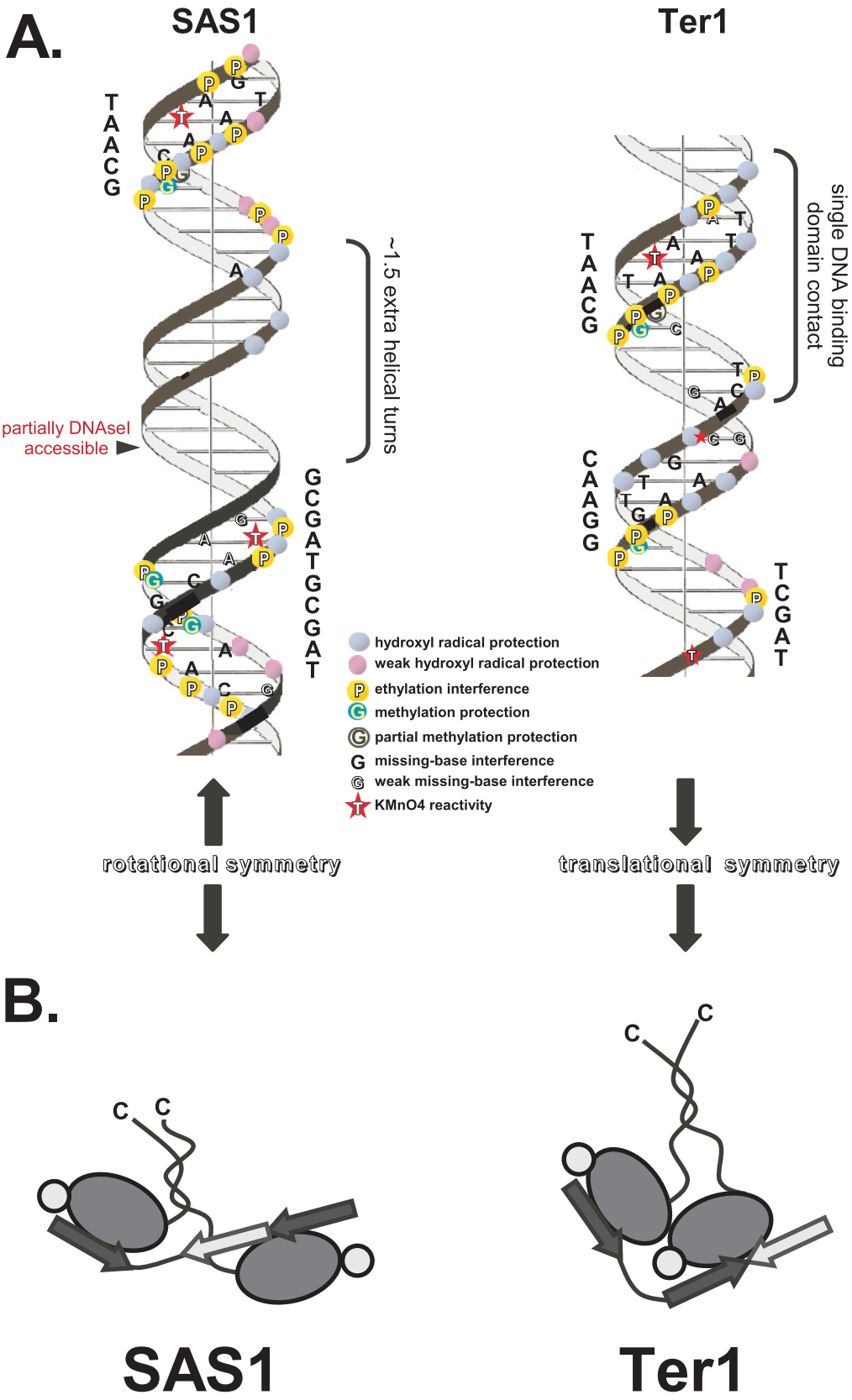

FIG. 7. Schematic representations of Sap1 bound to Ter1 versus SAS1. (A) Helical projections of SAS1 and Ter1 sites, summarizing locations of Sap1 base-specific and sugar-phosphate contacts, as well as sites of $KMnO_4$ reactivity. Note the alternate symmetries displayed by the subunits of the Sap1 dimer bound to Ter1 versus Sap1. (B) Models of Sap1-SAS1 and Sap1-Ter1 complexes.

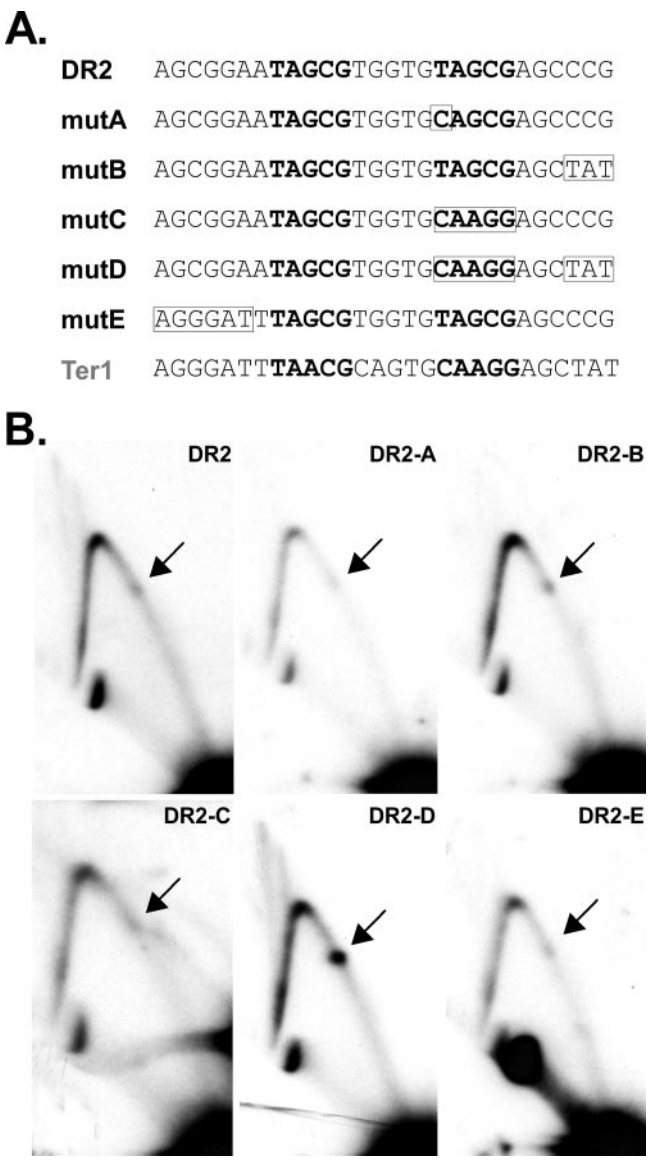

FIG. 8. Conversion of the nonnatural Sap1 binding site DR2 from an inefficient into an efficient replication fork barrier by modulation of the protein-DNA interactions of the fork-proximal Sap1 subunit. (A) Sequence comparison of DR2, Ter1, and the DR2 mutants analyzed (mutA, DR2-A mutant; mutB, DR2-B mutant; etc.). The core motifs are shown in bold, and mutated regions are boxed. (B) 2D gels of DR2 and DR2-A to DR2-E mutants. PvuII-digested replication intermediates of the respective plasmids were prepared as described in Materials and Methods. Note the weak fork barrier activity of DR2 (black arrow), which is dramatically increased in the DR2-D mutant.

the base pair contacts of Sap1 with the two sites (Fig. 2) are very similar, we were interested to determine which region of Ter1 conferred upon this site the ability to arrest forks more efficiently than DR2. We therefore mutated several regions of DR2 and analyzed the mutants for extrachromosomal replication fork arrest (Fig. 8A). We chose not to mutate motif a, as this region is crucial for recruitment of Sap1 to Ter1 (Fig. 4) and mutations in this region of Ter1 abolish stable Sap1 binding and fork arrest (34, 48). Two-dimensional gel analysis of the DR2 mutants revealed that only one of the mutants (the DR2-D mutant), in which motif b (TAGCG→CAAGG) as well as the region corresponding to motif c of Ter1 (AGCCC G→AGCTAT) has been altered to resemble the analogous bases of Ter1, was able to arrest replication efficiently. Mutating either of these regions individually had no effect on fork arrest (Fig. 8A and B). Interestingly, although we were unable to detect any base-specific contacts at motif c of Ter1 by the methods used (Fig. 2), this region appears to cooperate with motif b to cause efficient fork arrest. Because Sap1 makes several sugar-phosphate contacts with motif c of Ter1 (Fig. 5), we hypothesize that these contacts are critical for efficient fork arrest. In summary, the results suggest that modulating the interaction of the fork-proximal Sap1 subunit with its direct repeat-type binding site suffices to convert an inefficient fork barrier into an efficient one.

Relative affinities of various Sap1 binding sites. Several studies of prokaryotic systems have suggested that the mechanism of fork arrest is probably not explained simply by strong binding of the terminator proteins to their cognate sites (19, 21, 63), nor can DNA binding alone account for the polarity of the process (46, 52). In our system, the lack of fork arrest at SAS1 and the inefficient arrest at DR2 could theoretically be explainable by the decreased affinity of Sap1 for these sites compared to that for Ter1. Alternatively, striking or subtle architectural differences between the various Sap1 complexes may determine whether or not forks are blocked. In order to begin to distinguish between these possibilities, we determined the relative binding affinities of Sap1 bound to Ter1, DR2, DR2-D, or SAS1 by using comparative gel mobility shift assays. As shown in Fig. 9A, the binding curves of Sap1 bound to Ter1, DR2, and DR2-D are nearly identical. We approximated the relative K_d values from these curves by determining which concentrations of Sap1 resulted in half-maximal DNA binding. Accordingly, the mean half-maximal binding values (±standard deviations) of Sap1 to Ter1, DR2, and DR2-D were 5.5 (±1.4) nM, 2.6 (±0.5) nM, and 4.4 (±0.4) nM, respectively. As the results clearly show that the binding affinities of Sap1 for the sites are comparable, the relatively inefficient fork arrest at DR2 could not be explained by a lower affinity of Sap1 for this site than for Ter1. Similarly, the DR2-D mutation restored efficient fork arrest not simply by increasing the affinity of Sap1 for this site. The results are consistent with the aforementioned studies of prokaryotes and suggest that DNA binding affinity alone cannot account for the mechanism of Sap1-mediated replication fork arrest. The relative affinity of Sap1 for SAS1 was reduced ~7- to 8-fold compared to the affinity for the direct repeat-type sites, with an approximate K_d value of 37.2 (±8.9) nM (Fig. 9A), precluding conclusions about whether binding affinity and/or the architecture of the Sap1-SAS1 complex accounts for the lack of fork arrest at this site.

Subtle structural differences in the Sap1-Ter1 and Sap1-DR2 complexes. Because Sap1 demonstrates comparable binding affinities for Ter1 and DR2 (Fig. 9A) and recognizes the direct repeats of these sites in similar manners (Fig. 2C) but forks do not arrest efficiently at DR2 (Fig. 8B), we hypothesized that more-subtle structural differences between the complexes may exist. We therefore analyzed the interaction of Sap1 with DR2 by $KMnO_4$ probing. Indeed, Sap1 binding caused different $KMnO_4$ reactivities at the two sites (compare Fig. 6A and 9B, left panel). Specifically, Sap1 binding exposed

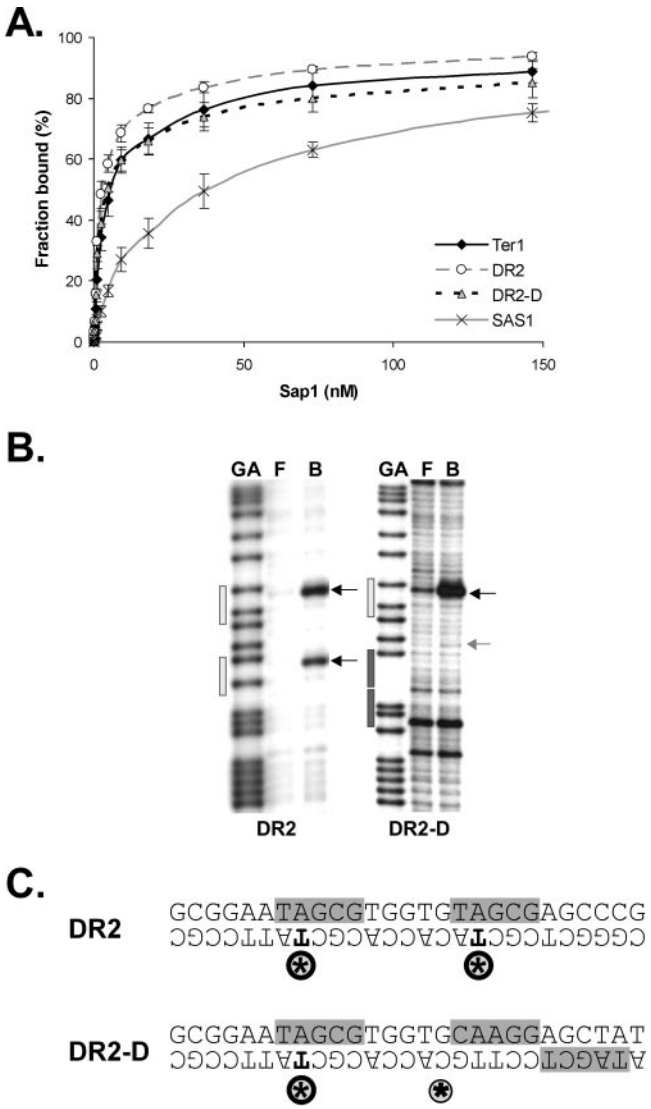

FIG. 9. Analysis of Sap1-DNA interaction at various binding sites reveals structural rearrangements without changes in binding affinity. (A) Binding curves of His_6-Sap1 bound to Ter1, DR2, the DR2-D mutant, or SAS1. (B) $KMnO_4$ probing of the bottom strands of DR2 and DR2-D. All lanes contained 20 fmol DNA probe. Lanes GA, G+A Maxam-Gilbert sequencing ladder; lanes F, uncomplexed (free) DNA; lanes B, DNA plus 80 ng His_6-Sap1. Locations of the core motifs and mutated motifs are denoted by light- and dark-gray boxes, respectively. (C) Summary of $KMnO_4$ probing of DR2 versus DR2-D. Symbols are described in the legend for Fig. 6.

two analogous second-position thymines in motifs a and b of the DR2 bottom strand (Fig. 9B, left panel), whereas only the thymine of motif a was exposed at Ter1 (Fig. 6A). In addition, the bottom-strand cytosine immediately preceding motif b of Ter1 and DR2 was susceptible to oxidation by $KMnO_4$ only in Ter1 and not in DR2 (compare Fig. 6A and 9B, left panel). Interestingly, the $KMnO_4$ reactivity of the DR2-D mutation resembles that of Sap1-Ter1 (compare Fig. 6A and 9B, right panel). In conjunction with the similar binding affinities of Sap1 for Ter1 and DR2, the results suggest that subtle binding differences and subsequent rearrangement of the respective protein-DNA complexes may determine, at least in part, whether efficient fork arrest occurs at these sites.

DISCUSSION

Although Sap1 binds both Ter1 (34, 48; this study) and SAS1 (3, 4) with relatively high sequence specificity, the DNA-protein interactions and therefore the architectures of the two complexes differ markedly. Comparative Ter1 DNase I footprinting of a single Sap1 subunit with that of the dimer (Fig. 2 and 4) suggests that major rearrangement of the complex must occur in order to accommodate the dimer due to space restrictions. In contrast, SAS1 allows for a more spacious arrangement of the Sap1 subunits. These results are consistent with our previous findings that Sap1 bends the Ter1 site to a greater extent than SAS1 (34). Importantly, whereas the head-to-tail arrangement of subunit binding at Ter1 results in a compact complex with translational symmetry, the subunits bind SAS1 with mirror image rotational symmetry. Because these sites have drastically different biological functions, it is interesting to speculate that the altered binding geometries at these sites allow for recruitment of a single protein to perform two different functions. As Sap1 is presumed also to bind DNA without sequence specificity in vivo in order to regulate DNA topology and maintain genome stability (18), it will be interesting to determine in which manner this binding occurs.

Sap1 binding induces conformational changes in its binding sites (Fig. 6 and 9B). As expected, these helical distortions reflect the mode of dimer binding. However, we were surprised to find that, although mild helical distortion was evident internal to motifs a and b of both Ter1 and SAS1, the major distorted regions were located within the core recognition motifs in all sites analyzed. Thus, protein binding apparently led to helical distortion directly at the site of subunit contact. Furthermore, the distortion was extremely localized, as even immediate thymine neighbors of the core motifs were unaltered as probed by $KMnO_4$ (Fig. 6A and C). The symmetry of distortion directly paralleled the symmetry of binding motifs, such that every second-position bottom-strand thymine of the sequence TAACG or TAGCG was modified regardless of which site was analyzed (Fig. 6 and 9B). These results suggest that $KMnO_4$ reactivity within the recognition motifs may be due to the mechanism of binding of the Sap1 DNA binding domain itself rather than to passive untwisting of the area during dimer binding. This would differ from the distortion induced between the motifs in Ter1 and SAS1 (but lacking at DR2), which is probably due to dimer-induced bending. The potential significance of these structural changes for fork arrest is discussed below. It is interesting to note that such localized $KMnO_4$ reactivity has been found to be due to a base-flipping mechanism in several methyltransferases and DNA repair enzymes (55, 61), suggesting that Sap1 may also flip out bases during binding. Alternatively, Sap1 may open the helix at the core motifs to insert contact elements.

We have demonstrated that nonnatural Sap1 binding site DR2, which is highly homologous in sequence to Ter1, binds Sap1 in a manner similar to Ter1 yet acts as only a very inefficient fork barrier in vivo (Fig. 8). Notably, the DNA binding affinities of Sap1 for these two sites are nearly identical, suggesting that binding affinity alone cannot explain the

differences in fork arrest. These results are consistent with similar evidence from prokaryotic systems (19, 24, 52, 63). Modulating the interaction of the replication fork-proximal Sap1 subunit with DR2 can convert this site from an inefficient to a very efficient replication fork barrier (DR2-D) (Fig. 8A). Again, binding affinities of Sap1 for DR2 versus DR2-D are nearly identical, suggesting that the mutations affect fork arrest by means other than enhancement of binding affinities. It is therefore interesting to note that Sap1 causes distinctly different $KMnO_4$ reactivities at Ter1 versus DR2 and that $KMnO_4$ reactivity at DR2-D is similar to that at Ter1. We hypothesize that, although the Sap1 dimer appears to bind both Ter1 and DR2 in architecturally similar configurations, subtle changes in the nature of the protein-DNA complex may determine whether or not forks are arrested. These structural changes could, in principle, lead to an altered DNA-protein complex that forms a more stable impediment to the oncoming replication fork. It is perhaps notable, therefore, that the mutations which increased fork-blocking efficiency of DR2 are located at the replication fork-proximal side of the complex. Binding-dependent structural changes could thus expose the Sap1-DNA complex to the oncoming replisome in a manner suitable to arrest fork progression, either through direct interaction with components of the replisome or more indirectly. Such DNA binding-induced allosteric protein-DNA conformational changes have been suggested to modulate transcription factor function (40). Bacterial terminator proteins block fork progression by inhibiting replicative helicases (29, 39). This is accomplished through both protein-DNA and protein-protein interactions of the terminator proteins with the replicative helicase (46, 51, 52). It will be interesting to determine whether eukaryotic fork-blocking proteins, such as Sap1, also act as contrahelicases and whether this is dependent on the structural context.

Most prokaryotic and eukaryotic replication fork barriers, including Ter1, are polar in nature. In bacteria, polarity is generated by the assembly of a functionally asymmetric terminator-protein complex (reviewed in reference 6). For instance, both RTP and Tus, the terminator proteins of *B. subtilis* and *E. coli*, respectively, are situated on the DNA to make specific contacts with the oncoming replicative helicase of the replisome from only one orientation (46, 52, 62). In addition, the crystal structure of the Tus-Ter complex reveals asymmetric backbone contacts (27), and RTP, which requires cooperative binding of two dimers to its binding site in order to cause fork arrest (41, 58), makes asymmetric nucleoside contacts with the fork-proximal and fork-distal halves of the Ter site (38). Although we have not detected any notable asymmetry in the DNA-protein contacts of the Sap1-Ter1 complex, DNA ligand-induced asymmetry of the protein could still generate polarity. In this respect, it is interesting to note that the Sap1 subunits arrange themselves into a complex with translational symmetry (Fig. 7), resulting in a structurally polar complex. The replication fork approaches Ter1 in situ from the side containing motif c, so the fork would encounter drastically different faces of the fork-pausing complex depending on the direction from which it approached the site. Future experiments should address whether the blocking-competent complex achieves polarity by direct interactions of the fork-proximal subunit with a component of the oncoming replisome or whether the mechanism of polarity generation is more indirect.

ACKNOWLEDGMENTS

This work was supported by grants from the National Institute of Allergy and Infectious Diseases and the National Institute of General Medical Sciences.

REFERENCES

1. **Ahn, J. S., F. Osman, and M. C. Whitby.** 2005. Replication fork blockage by RTS1 at an ectopic site promotes recombination in fission yeast. EMBO J. **24:**2011–2023.
2. **Arcangioli, B., T. D. Copeland, and A. J. Klar.** 1994. Sap1, a protein that binds to sequences required for mating-type switching, is essential for viability in *Schizosaccharomyces pombe*. Mol. Cell. Biol. **14:**2058–2065.
3. **Arcangioli, B., M. Ghazvini, and V. Ribes.** 1994. Identification of the DNA-binding domains of the switch-activating-protein Sap1 from S. pombe by random point mutations screening in E. coli. Nucleic Acids Res. **22:**2930–2937.
4. **Arcangioli, B., and A. J. Klar.** 1991. A novel switch-activating site (SAS1) and its cognate binding factor (SAP1) required for efficient mat1 switching in Schizosaccharomyces pombe. EMBO J. **10:**3025–3032.
5. **Bada, M., D. Walther, B. Arcangioli, S. Doniach, and M. Delarue.** 2000. Solution structural studies and low-resolution model of the Schizosaccharomyces pombe sap1 protein. J. Mol. Biol. **300:**563–574.
6. **Bastia, D., and B. K. Mohanty.** 2006. Termination of DNA replication, p. 155–174. *In* M. L. DePamphilis (ed.), DNA replication and human disease. Cold Spring Harbor Laboratory Press, Cold Spring Harbor, N.Y.
7. **Boddy, M. N., and P. Russell.** 2001. DNA replication checkpoint. Curr. Biol. **11:**R953–R956.
8. **Brewer, B. J., D. Lockshon, and W. Fangman.** 1992. The arrest of replication forks in the rDNA of yeast occurs independently of transcription. Cell **71:**267–271.
9. **Brunelle, A., and R. F. Schleif.** 1987. Missing contact probing of DNA-protein interactions. Proc. Natl. Acad. Sci. USA **84:**6673–6676.
10. **Bussiere, D. E., and D. Bastia.** 1999. Termination of DNA replication of bacterial and plasmid chromosomes. Mol. Microbiol. **31:**1611–1618.
11. **Bussiere, D. E., D. Bastia, and S. W. White.** 1995. Crystal structure of replication terminator protein of B. subtilis at 2.6 Å. Cell **80:**651–660.
12. **Calzada, A., B. Hodgson, M. Kanemaki, A. Bueno, and K. Labib.** 2005. Molecular anatomy and regulation of a stable replisome at a paused eukaryotic DNA replication fork. Genes Dev. **19:**1905–1919.
13. **Chandrashekaran, S., U. H. Manjunatha, and V. Nagaraja.** 2004. KpnI restriction endonuclease and methyltransferase exhibit contrasting mode of sequence recognition. Nucleic Acids Res. **32:**3148–3155.
14. **Coskun-Ari, F. F., and T. M. Hill.** 1997. Sequence-specific interactions in the Tus-Ter complex and the effect of base pair substitutions on arrest of DNA replication in Escherichia coli. J. Biol. Chem. **272:**26448–26456.
15. **Dalgaard, J. Z., and A. J. Klar.** 2001. A DNA replication-arrest site RTS1 regulates imprinting by determining the direction of replication at mat1 in S. pombe. Genes Dev. **15:**2060–2068.
16. **Dalgaard, J. Z., and A. J. Klar.** 2000. swi1 and swi3 perform imprinting, pausing, and termination of DNA replication in S. pombe. Cell **102:**745–751.
17. **Defossez, P. A., R. Prusty, M. Kaeberlein, S. J. Lin, P. Ferrigno, P. A. Silver, R. L. Keil, and L. Guarente.** 1999. Elimination of replication block protein Fob1 extends the life span of yeast mother cells. Mol. Cell **3:**447–455.
18. **de Lahondes, R., V. Ribes, and B. Arcangioli.** 2003. Fission yeast Sap1 protein is essential for chromosome stability. Eukaryot. Cell **2:**910–921.
19. **Duggin, I. G., J. M. Matthews, N. E. Dixon, R. G. Wake, and J. P. Mackay.** 2005. A complex mechanism determines polarity of DNA replication fork arrest by the replication terminator complex of Bacillus subtilis. J. Biol. Chem. **280:**13105–13113.
20. **Gambus, A., R. C. Jones, A. Sanchez-Diaz, M. Kanemaki, F. van Deursen, R. D. Edmondson, and K. Labib.** 2006. GINS maintains association of Cdc45 with MCM in replisome progression complexes at eukaryotic DNA replication forks. Nat. Cell Biol. **8:**358–366.
21. **Gautam, A., and D. Bastia.** 2001. A replication terminus located at or near a replication checkpoint of Bacillus subtilis functions independently of stringent control. J. Biol. Chem. **276:**8771–8777.
22. **Gerber, J. K., E. Gogel, C. Berger, M. Wallisch, F. Muller, I. Grummt, and F. Grummt.** 1997. Termination of mammalian rDNA replication: polar arrest of replication fork movement by transcription termination factor TTF-I. Cell **90:**559–567.
23. **Ghazvini, M., V. Ribes, and B. Arcangioli.** 1995. The essential DNA-binding protein sap1 of *Schizosaccharomyces pombe* contains two independent oligomerization interfaces that dictate the relative orientation of the DNA-binding domain. Mol. Cell. Biol. **15:**4939–4946.
24. **Henderson, T. A., A. F. Nilles, M. Valjavec-Gratian, and T. M. Hill.** 2001. Site-directed mutagenesis and phylogenetic comparisons of the Escherichia

coli Tus protein: DNA-protein interactions alone can not account for Tus activity. Mol. Genet. Genomics **265:**941–953.
25. **Huberman, J. A., L. D. Spotila, K. A. Nawotka, S. M. el-Assouli, and L. R. Davis.** 1987. The in vivo replication origin of the yeast 2 microns plasmid. Cell **51:**473–481.
26. **Johzuka, K., and T. Horiuchi.** 2002. Replication fork block protein, Fob1, acts as an rDNA region specific recombinator in S. cerevisiae. Genes Cells **7:**99–113.
27. **Kamada, K., T. Horiuchi, K. Ohsumi, M. Shimamoto, and K. Morikawa.** 1996. Structure of a replication terminator protein complexed with DNA. Nature **383:**598–603.
28. **Kaykov, A., A. M. Holmes, and B. Arcangioli.** 2004. Formation, maintenance and consequences of the imprint at the mating-type locus in fission yeast. EMBO J. **23:**930–938.
29. **Khatri, G. S., T. MacAllister, P. R. Sista, and D. Bastia.** 1989. The replication terminator protein of E. coli is a DNA sequence-specific contra-helicase. Cell **59:**667–674.
30. **Kobayashi, T.** 2003. The replication fork barrier site forms a unique structure with Fob1p and inhibits the replication fork. Mol. Cell. Biol. **23:**9178–9188.
31. **Kobayashi, T., D. J. Heck, M. Nomura, and T. Horiuchi.** 1998. Expansion and contraction of ribosomal DNA repeats in Saccharomyces cerevisiae: requirement of replication fork blocking (Fob1) protein and the role of RNA polymerase I. Genes Dev. **12:**3821–3830.
32. **Kobayashi, T., and T. Horiuchi.** 1996. A yeast gene product, Fob1 protein, required for both replication fork blocking and recombinational hotspot activities. Genes Cells **1:**465–474.
33. **Kralicek, A. V., P. K. Wilson, G. B. Ralston, R. G. Wake, and G. F. King.** 1997. Reorganization of terminus DNA upon binding replication terminator protein: implications for the functional replication fork arrest complex. Nucleic Acids Res. **25:**590–596.
34. **Krings, G., and D. Bastia.** 2005. Sap1p binds to Ter1 at the ribosomal DNA of Schizosaccharomyces pombe and causes polar replication fork arrest. J. Biol. Chem. **280:**39135–39142.
35. **Krings, G., and D. Bastia.** 2004. swi1- and swi3-dependent and independent replication fork arrest at the ribosomal DNA of Schizosaccharomyces pombe. Proc. Natl. Acad. Sci. USA **101:**14085–14090.
36. **Lambert, S., and A. M. Carr.** 2005. Checkpoint responses to replication fork barriers. Biochimie **87:**591–602.
37. **Lambert, S., A. Watson, D. M. Sheedy, B. Martin, and A. M. Carr.** 2005. Gross chromosomal rearrangements and elevated recombination at an inducible site-specific replication fork barrier. Cell **121:**689–702.
38. **Langley, D. B., M. T. Smith, P. J. Lewis, and R. G. Wake.** 1993. Protein-nucleoside contacts in the interaction between the replication terminator protein of B. subtilis and the DNA terminator. Mol. Microbiol. **10:**771–779.
39. **Lee, E. H., A. Kornberg, M. Hidaka, T. Kobayashi, and T. Horiuchi.** 1989. Escherichia coli replication termination protein impedes the action of helicases. Proc. Natl. Acad. Sci. USA **86:**9104–9108.
40. **Lefstin, J. A., and K. R. Yamamoto.** 1998. Allosteric effects of DNA on transcriptional regulators. Nature **392:**885–888.
41. **Lewis, P. J., G. B. Ralston, R. I. Christopherson, and R. G. Wake.** 1990. Identification of the replication terminator binding sites in the terminus region of the B. subtilis chromosome and stoichiometry of the binding. J. Mol. Biol. **214:**73–84.
42. **Linskens, M. H. K., and J. A. Huberman.** 1988. Organization of replication of ribosomal DNA in *Saccharomyces cerevisiae*. Mol. Cell. Biol. **8:**4927–4935.
43. **Little, R. D., T. H. Platt, and C. L. Schildkraut.** 1993. Initiation and termination of DNA replication in human rRNA genes. Mol. Cell. Biol. **13:**6600–6613.
44. **Lopez-Estrano, C., J. B. Schvartzman, D. B. Krimer, and P. Hernandez.** 1999. Characterization of the pea rDNA replication fork barrier: putative cis-acting and trans-acting factors. Plant Mol. Biol. **40:**99–110.
45. **Lopez-Estrano, C., J. B. Schvartzman, D. B. Krimer, and P. Hernandez.** 1998. Co-localization of polar replication fork barriers and rRNA transcription terminators in mouse rDNA. J. Mol. Biol. **277:**249–256.
46. **Manna, A. C., K. S. Pai, D. E. Bussiere, and D. Bastia.** 1996. Helicase-contrahelicase interaction and the mechanism of termination of DNA replication. Cell **87:**881–891.
47. **McGlynn, P., and R. G. Lloyd.** 2002. Recombinational repair and restart of damaged replication forks. Nat. Rev. Mol. Cell. Biol. **3:**859–870.
48. **Mejia-Ramirez, E., A. Sanchez-Gorostiaga, D. B. Krimer, J. B. Schvartzman, and P. Hernandez.** 2005. The mating type switch-activating protein Sap1 is required for replication fork arrest at the rRNA genes of fission yeast. Mol. Cell. Biol. **25:**8755–8761.
49. **Mohanty, B. K., N. K. Bairwa, and D. Bastia.** 2006. The Tof1p-Csm3p protein complex counteracts the Rrm3p helicase to control replication termination of Saccharomyces cerevisiae. Proc. Natl. Acad. Sci. USA **103:**897–902.
50. **Mohanty, B. K., and D. Bastia.** 2004. Binding of the replication terminator protein Fob1p to the Ter sites of yeast causes polar fork arrest. J. Biol. Chem. **279:**1932–1941.
51. **Mohanty, B. K., D. E. Bussiere, T. Sahoo, K. S. Pai, W. J. Meijer, S. Bron, and D. Bastia.** 2001. Structural and functional analysis of a bipolar replication terminus. Implications for the origin of polarity of fork arrest. J. Biol. Chem. **276:**13160–13168.
52. **Mulugu, S., A. Potnis, Shamsuzzaman, J. Taylor, K. Alexander, and D. Bastia.** 2001. Mechanism of termination of DNA replication of Escherichia coli involves helicase-contrahelicase interaction. Proc. Natl. Acad. Sci. USA **98:**9569–9574.
53. **Neylon, C., A. V. Kralicek, T. M. Hill, and N. E. Dixon.** 2005. Replication termination in *Escherichia coli*: structure and antihelicase activity of the Tus-Ter complex. Microbiol. Mol. Biol. Rev. **69:**501–526.
54. **Papp, P. P., and D. K. Chattoraj.** 1994. Missing-base and ethylation interference footprinting of P1 plasmid replication initiator. Nucleic Acids Res. **22:**152–157.
55. **Roberts, R. J., and X. Cheng.** 1998. Base flipping. Annu. Rev. Biochem. **67:**181–198.
56. **Rothstein, R., B. Michel, and S. Gangloff.** 2000. Replication fork pausing and recombination or "gimme a break". Genes Dev. **14:**1–10.
57. **Rubin, C. M., and C. W. Schmid.** 1980. Pyrimidine-specific chemical reactions useful for DNA sequencing. Nucleic Acids Res. **8:**4613–4619.
58. **Sahoo, T., B. K. Mohanty, and D. Bastia.** 1995a. Termination of DNA replication in vitro. EMBO J. **14:**619–628.
59. **Sanchez, J. A., S. M. Kim, and J. A. Huberman.** 1998. Ribosomal DNA replication in the fission yeast, Schizosaccharomyces pombe. Exp. Cell Res. **238:**220–230.
60. **Sanchez-Gorostiaga, A., C. Lopez-Estrano, D. B. Krimer, J. B. Schvartzman, and P. Hernandez.** 2004. Transcription termination factor reb1p causes two replication fork barriers at its cognate sites in fission yeast ribosomal DNA in vivo. Mol. Cell. Biol. **24:**398–406.
61. **Serva, S., E. Weinhold, R. J. Roberts, and S. Klimasauskas.** 1998. Chemical display of thymine residues flipped out by DNA methyltransferases. Nucleic Acids Res. **26:**3473–3479.
62. **Sista, P. R., C. A. Hutchinson III, and D. Bastia.** 1991. DNA-protein interaction at the replication termini of plasmid R6K. Genes Dev. **5:**74–82.
63. **Skokotas, A., M. Wrobelski, and T. Hill.** 1994. Isolation and characterization of mutants of Tus, the replication arrest protein of Escherichia coli. J. Biol. Chem. **269:**20446–20455.
64. **Takeuchi, Y., T. Horiuchi, and T. Kobayashi.** 2003. Transcription-dependent recombination and the role of fork collision in yeast rDNA. Genes Dev. **17:**1497–1506.
65. **Tourriere, H., G. Versini, V. Cordon-Preciado, C. Alabert, and P. Pasero.** 2005. Mrc1 and Tof1 promote replication fork progression and recovery independently of Rad53. Mol. Cell **19:**699–706.
66. **Wiesendanger, B., R. Lucchini, T. Koller, and J. M. Sogo.** 1994. Replication fork barriers in the Xenopus rDNA. Nucleic Acids Res. **22:**5038–5046.
67. **Wilce, J. A., J. P. Vivian, A. F. Hastings, G. Otting, R. H. Folmer, I. G. Duggin, R. G. Wake, and M. C. Wilce.** 2001. Structure of the RTP-DNA complex and the mechanism of polar replication fork arrest. Nat. Struct. Biol. **8:**206–210.
68. **Zhao, A., A. Guo, Z. Liu, and L. Pape.** 1997. Molecular cloning and analysis of Schizosaccharomyces pombe Reb1p: sequence-specific recognition of two sites in the far upstream rDNA intergenic spacer. Nucleic Acids Res. **25:**904–910.